Lossless Authentication Watermarking Based on Adaptive Modular Arithmetic

Hengfu YANG [1,2], *Xingming SUN* [1], *Guang SUN* [1,3], *Zuwei TIAN* [1,2]

[1]School of Computer and Communication, Hunan University, No. 252, Lushan South Road, Changsha, 410082, China
[2]Dept of Information Science & Engg., Hunan First Normal Univ., No. 1015, Fenglin 3rd Road, Changsha, 410205, China
[3]Information Management Dept., Hunan Fin. & Economic College, No. 139, Fenglin 2nd Road, Changsha, 410205, China

sunnudt@163.com, hengfuyang@hotmail.com, hengfuyang@163.com

Abstract. *Reversible watermarking schemes based on modulo-256 addition may cause annoying salt-and-pepper noise. To avoid the salt-and-pepper noise, a reversible watermarking scheme using human visual perception characteristics and adaptive modular arithmetic is proposed. First, a high-bit residual image is obtained by extracting the most significant bits (MSB) of the original image, and a new spatial visual perception model is built according to the high-bit residual image features. Second, the watermark strength and the adaptive divisor of modulo operation for each pixel are determined by the visual perception model. Finally, the watermark is embedded into different least significant bits (LSB) of original image with adaptive modulo addition. The original image can be losslessly recovered if the stego-image has not been altered. Extensive experiments show that the proposed algorithm eliminates the salt-and-pepper noise effectively, and the visual quality of the stego-image with the proposed algorithm has been dramatically improved over some existing reversible watermarking algorithms. Especially, the stego-image of this algorithm has about 9.9864 dB higher PSNR value than that of modulo-256 addition based reversible watermarking scheme.*

Keywords

Adaptive modular arithmetic, salt-and-pepper noise, lossless watermarking, visual perception.

1. Introduction

Common irreversible watermarking techniques [1-4] introduce some amount of distortion to the original image and the distortion is permanent and not reversible. There are, however, some applications (such as medical, astronomical, and military image systems) where any distortion introduced to the image is not acceptable [5]. In these above fields, it is expected to reverse the marked media back to the original cover media after the hidden data are retrieved for some legal or other considerations [5-7]. In

order to avoid permanent distortion, a new branch of the watermarking technique, called reversible, distortion-free, or lossless watermarking, has been developed. In fact, Barton's patent, filed in 1994, may be the earliest one [8]. Recently, a number of lossless data hiding algorithms have been reported in the literature, and attention on lossless data hiding scheme are increasing [8-22]. According to embedding strategies, reversible data hiding schemes can be classified into four types. The first type of algorithm losslessly compressed selected features from the original image to obtain enough space, which were then replaced with the watermark payload [9-11]. But the capacity depended on the adopted image compress algorithm. The second type of reversible scheme used difference expansion to embed information [12-14]. The main advantage was high embedding capacity, but this type of algorithm was lack of capacity control due to embedding of a location map which contained the location information of all selected expandable difference values. The third types of algorithms are lossless data hiding techniques based on histogram modification [15-17]. They used image histogram to hide message bits and achieve reversibility. This type of algorithm had low computational cost because that there were no need any transform for data embedding, all processes are performed in spatial domain in most histogram-based methods, but the embedding capacity of this type is low. The fourth type of algorithm is the method based on modular arithmetic [18-22]. This type of reversible watermarking algorithms used modulo addition (say modulo-256 addition) to embed the watermark into the original watermark. The type of algorithm had low computational consumption, but it cased annoying salt-and-pepper noise in the stego-image.

This paper focused on lossless data hiding method based on modular arithmetic. Honsinger et al. [18] presented a lossless fragile watermarking technique for image authentication by applying modulo-256 addition. But this method may introduce visual artifacts, similar to salt-and-pepper noise, into the watermarked image when pixels with grayscales close to zero are flipped to values close to 255 and vice versa. Macq [19] described a modification to the patchwork algorithm [23] to achieve lossless watermark

embedding which uses modulo-256 addition. However, this method also suffers from annoying salt-and-pepper noise. De Vleeschouwer et al. [20] proposed a lossless data embedding algorithm based on patchwork theory [23], which eliminated salt-and-pepper noise by adopting circle interpretation of bijective transformations, but the embedding capacity of the scheme is low. Similarly, S. Weng et al. [21] utilized symmetric modulo operation to avoid salt-and-pepper artifacts, but this method has embedded capacity because the cover image may have some useless blocks which cannot be used to embed the watermark. In a word, the watermarking scheme with modulo operations has two main defects: perceptible artifacts in the form of salt-and-pepper noise are easily introduced into the watermarked image and the degradation of watermark detection especially on images whose histograms are relatively spread from the values from 0 to 255 [22].

In order to avoid salt-and-pepper visual artifacts caused by modulo-256 addition based lossless watermarking algorithms and to provide good perceptual transparency, we exploit visual perception characteristics and adaptive modular arithmetic to achieve a reversible watermarking scheme (called the AMA method hereafter) in this paper.

2. Visual Perception Model and the Adaptive Divisor

It is known that the robustness and the imperceptibility of the watermark are contradictory to each other. The best method to achieve the tradeoff between the aforementioned two requirements is to take the human visual perception into account while embedding the watermark [24-27]. Jiying Zhao et al. [24] developed an image spatial masking by employing the brightness, edges, and region activities. Dušan Levický et al. [25] briefly described four HVS (Human Visual System) models used in image processing applications such as digital image watermarking, and concluded that the exploiting of HVS models can achieve a very good tradeoff between perceptual transparency and robustness of embedded watermarks. But the existing HVS models did not take full advantage of the human visual perception characteristics, and there are many parameters need setting for HVS computation. In this paper, we make use of the image features, including the luminance masking, texture masking and edge masking, to create a new spatial visual perception model, and then use the model to deduce an adaptive divisor for reversible watermarking based on adaptive modular arithmetic.

To eliminate the salt-and-pepper noise caused by the modular arithmetic-based reversible watermarking, in the proposed scheme we only use adaptive least significant bits for each pixel to apply modular arithmetic (called adaptive modular arithmetic).

As to luminance masking, Lewis and Knowles assumed that human eyes usually have different sensitivity to different luminance, specifically, more sensitivity to noise in the areas with middle level luminance, and less sensitivity to noise in those areas with high and low brightness [28]. As a result, the calculation of luminance masking can be formulated as

$$\alpha(i,j) = \frac{\left|x(i,j)-127.5\right|}{127.5}. \tag{1}$$

where $x(i,j)$ is the pixel value at the spatial position (i,j) in the host image $\boldsymbol{I}$.

On the one hand, human eyes are more sensitive to the noise in smooth image areas, but less sensitive to that in texture image areas. On the other hand, the smooth image regions have small entropy value, while the texture image areas have big entropy value. In fact, entropy value is usually used to represent the texture feature [29,30]. Hence, we can use the entropy value of the sliding window as the texture masking (All the calculations are based on the image block of size $(2l+1)\times(2l+1)$, therefore in the implementation, we will use a sliding window of size $(2l+1)\times(2l+1)$, where $1 \leq l \leq 4$). Let $H(i,j)$ be the entropy of sub-block centered by the pixel $I(i,j)$. The entropy $H(i,j)$ can therefore be used to depict the texture characteristics of the pixel $I(i,j)$. This maximum entropy is achievable when all of the gray-levels have the same probability. In other words, an image block receives its maximum entropy when it contains the same number of all of the gray values in that block. For a 256-level image block with size of $(2l+1)\times(2l+1)$, the maximum entropy $H_{\max}$ is evaluated by

$$H_{\max} = -\sum_{i=-l}^{l}\sum_{j=-l}^{l}\frac{1}{(2l+1)^2}\log_2\left(\frac{1}{(2l+1)^2}\right) = 2\log_2(2l+1). \tag{2}$$

So, the normalized entropy $\beta(i,j)$ can be obtained by the following formula

$$\beta(i,j) = H(i,j)/H_{\max}. \tag{3}$$

As for edge masking, human eyes are very sensitive to the information distortion in the edge image area. Hence the watermark embedding must not lead to significant distortion in that image area. Image area with prominent edges has larger variance value, while smooth image area has smaller variance value. We can therefore use the variance of the image blocks to indicate the edge feature. Using the monotonic logarithm function for range compression we achieve the following expression for the edge masking.

$$V'(i,j) = \log_{10}(V(i,j)). \tag{4}$$

where $V(i,j)$ is the variance of the image block centered by the pixel $I(i,j)$. The maximum variance is in the block with a checkerboard pattern with the adjacent pixels having the

maximum and minimum permissible gray value. The maximum variance V_{max} is defined as

$$V_{max} = \frac{\left(2l^2 + 2l\right)\left(2l^2 + 2l + 1\right)}{\left(2l + 1\right)^4} G^2$$

$$< \left(\frac{\left(2l^2 + 2l + \frac{1}{2}\right)}{\left(2l + 1\right)^2} G\right)^2 = \left(\frac{G}{2}\right)^2. \tag{5}$$

where G is the maximum permissible gray value.

Then the normalized edge masking $\gamma(i,j)$ can be defined as

$$\gamma(i,j) = \frac{V'(i,j)}{\log_{10}(V_{max})} = \frac{\log_{10}(V(i,j))}{\log_{10}(G/2)^2}. \tag{6}$$

A large entropy value corresponds to the texture or edge image area, and the texture masking created by the entropy value also includes the image edge parts. While sharp edges play an important role in human spatial vision [31], so we must ensure low watermark strength to be embedded in the image edge areas to prevent the watermark embedding from corrupting the edge easily and causing severe distortion to the host image. Based on all the above considerations, the effect of visual perception characteristics is estimated by the formula

$$\tau(i,j) = \alpha(i,j) \times \left(\beta(i,j) - \gamma(i,j)\right). \tag{7}$$

At last, in order to improve the watermark invisibility and to enhance the controllability of the strength of the embedded watermark, we obtain the final visual perception factor (used as watermark strength) as follows by normalizing the visual perception effect $\tau(i,j)$.

$$\omega(i,j) = round\left\{\left(2^{(8-r)} - 1 - 1\right) \times \frac{\tau(i,j) - min(\tau)}{max(\tau) - min(\tau)} + 1\right\}. \tag{8}$$

where $1 \leq r \leq 7$ and r represents the MSBs number of each pixel used to calculate the visual perception masking. Function round(z) returns the nearest integer to the argument z, and max(z) and min(z) returns the maximum and minimum of the array z respectively. The factor $\omega(i,j)$ is the final visual perception factor of the pixel $I(i,j)$, and $1 \leq \omega(i,j) \leq 2^{(8-r)} - 1$.

After final perception factor has been obtained, the adaptive LSBs number $\lambda(i,j)$ in pixel $I(i,j)$ for modular addition operation can be derived as

$$\lambda(i,j) = \left\lfloor \log_2\left(\omega(i,j)\right) \right\rfloor + 1. \tag{9}$$

where $\lfloor z \rfloor$ denotes the floor function meaning "the greatest integer less than or equal to the real number z". The adaptive LSBs number $\lambda(i,j)$ satisfies $1 \leq \lambda(i,j) \leq 8\text{-}r$ because of (8).

At last, the adaptive divisor $\Phi(i,j)$ of pixel $I(i,j)$ for modular arithmetic during data embedding can be computed by

$$\phi(i,j) = 2^{\lambda(i,j)}. \tag{10}$$

Taking Peppers, Lena, Bone, and Baboon images for example, Fig. 1 illustrates the magnified visual perception factor. The darker region is considered visually less sensitive to noise and has relatively lower masking values. Meanwhile, the white part in the masking image is more sensitive to distortion and has higher masking values. From Fig. 1, we see that the highly-textured image regions or regions with higher and lower brightness have bigger masking values, while the smooth image areas and the prominent edge areas have lower values, indicating the proposed visual perception model can well depict the visual perception characteristics of the host images.
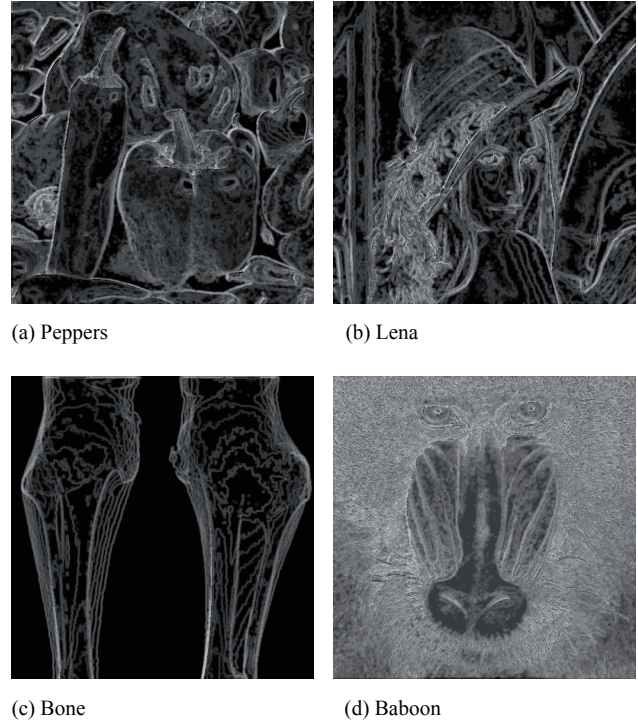

(a) Peppers   (b) Lena

(c) Bone   (d) Baboon

Fig. 1. Visual perception effect of Lena, Bone, and Baboon images magnified by 15 times.

Tab. 1 lists the distribution of the adaptive LSBs number $\lambda(i,j)$ for 4 test images: Peppers, Lena, Bone, and Baboon. From Tab. 1, it can be seen that the distribution of the adaptive LSBs number $\lambda(i,j)$ depends on image structure. Images with rich texture possess relatively more high-order LSBs for data embedding.

test images	adaptive LSBs number $\lambda(i,j)$			
	$\lambda(i,j) = 1$	$\lambda(i,j) = 2$	$\lambda(i,j) = 3$	$\lambda(i,j) = 4$
Peppers	28574	93186	121846	18538
Lena	50153	71725	115242	25024
Bone	159216	41054	56994	4880
Baboon	8	373	107735	154028

Tab. 1. The distribution of the adaptive LSBs number $\lambda(i,j)$ for 4 test images: Peppers, Lena, Bone, and Baboon.

3. Lossless Watermarking Scheme Based on Adaptive Modular Arithmetic

3.1 Lossless Data Embedding

To eliminate the salt-and-pepper noise artifacts, we use adaptive LSBs of each pixel (not all the bits) for watermark embedding. Reversibility is achieved by adaptive modulo addition. The watermark embedding procedure is illustrated in Fig. 2 and the detailed embedding algorithm is described as follows.
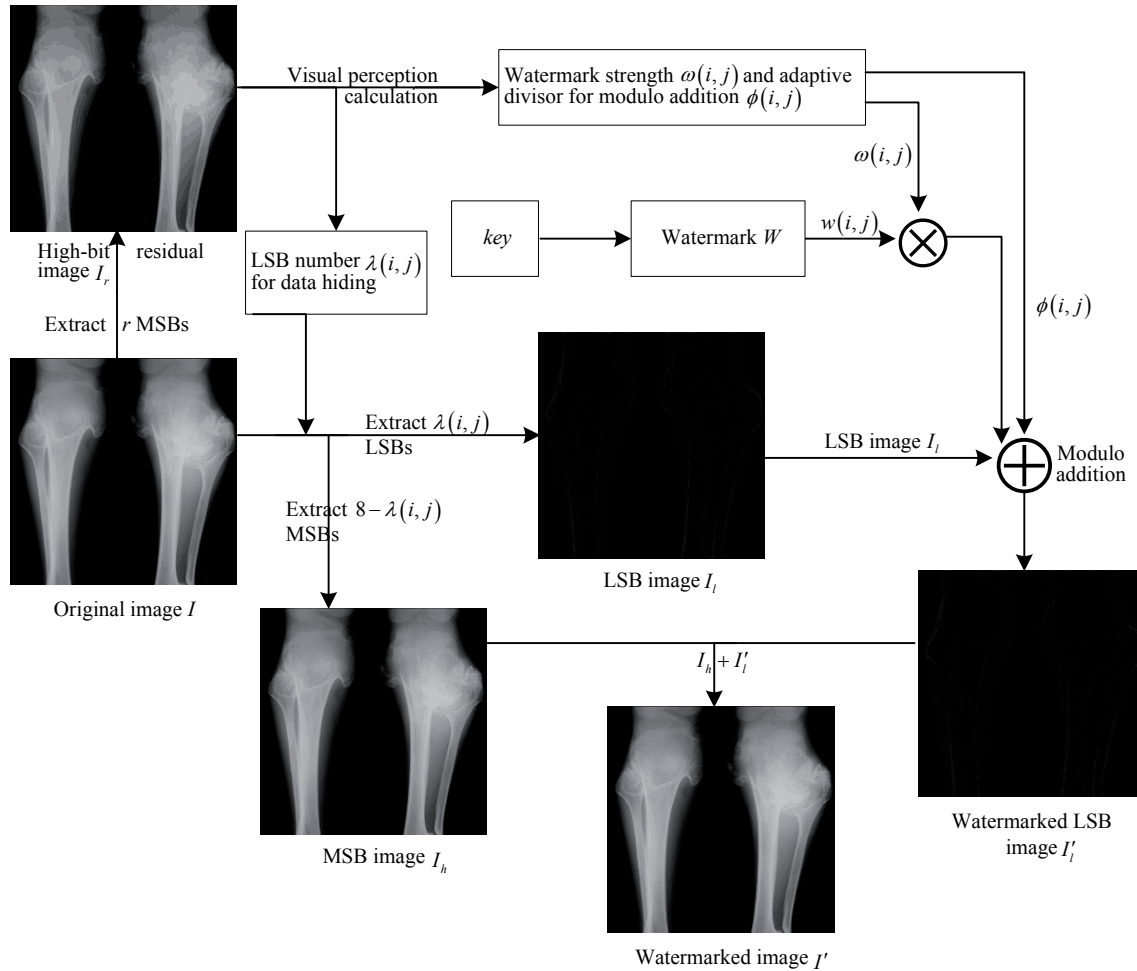

Fig. 2. The watermark embedding procedure

Input: Original image I of size $m \times n$, secret key k, and MSBs number r for visual perception calculation.

Output: watermarked image I' of size $m \times n$.

Step 1: Extract r (say 4) MSBs of the original image I to obtain its corresponding high-bit residual image I_r.

Step 2: Compute the final visual perception factor $\omega(i,j)$ from the high-bit residual image I_r using (8), and then use (9) to derive the adaptive LSBs number $\lambda(i,j)$ in pixel $I(i,j)$ for modular addition operation.

Step 3: Obtain the adaptive divisor $\Phi(i,j)$ of pixel $I(i,j)$ for modular arithmetic by (10).

Step 4: Produce the LSB image I_l and the MSB image I_h of original image by extracting $\lambda(i,j)$ LSBs and $8 - \lambda(i,j)$

MSBs of the pixel $I(i,j)$ respectively.

Step 5: Generate a pseudo random sequence **PN** with number 1 and -1 by secret key k as the watermark sequence **W**.

$$W = \left\{ w(i,j) \big| w(i,j) \in \{-1,1\}, 0 \le i < m, 0 \le j < n \right\}. \quad (11)$$

Step 6: Embed the watermark into the LSB image I_l by adaptive modular addition operation to generate the watermarked LSB image I_l',

$$I_l'(i,j) = \big(I_l(i,j) + \omega(i,j) \times w(i,j)\big) \bmod \phi(i,j). \quad (12)$$

Step 7: obtain the watermarked image I' by adding the MSB image I_h to the LSB image I_l'.

$$I' = I_h + I_l'. \quad (13)$$

3.2 Recovery of the Original Image and Watermark Detection

The procedure of recovering the original image is the inverse operation of the embedding process, and can be presented below.

Input: Watermarked image I', and secret key k, and MSBs number r for visual perception calculation.

Output: Original image I.

Step 1: Extract r MSBs from the watermarked image I' to obtain the high-bit residual image I_r', note that I_r' is the same as I_r because that the watermark is not embedded into the r MSBs of each pixel.

Step 2: By using the similar method in the Step 2 and Step 3 of the watermark insertion process, we can obtain the final visual perception factor $\omega(i,j)$, the adaptive LSBs number $\lambda(i,j)$ and the adaptive advisor $\Phi(i,j)$ of pixel $I'(i,j)$ for modular arithmetic according to the high-bit residual image I_r'.

Step 3: Generate the LSB image I_l' and the MSB image I_h' of original image by extracting $\lambda(i,j)$ LSBs and 8- $\lambda(i,j)$ MSBs of the pixel $I'(i,j)$ respectively.

Step 4: Use the shared secret key k to generate a pseudo random sequence PN with number 1 and -1 as the watermark signal W.

Step 5: Obtain the original LSB image I_l by the following formula.

$$I_l(i,j) = \left(I_l'(i,j) - \omega(i,j) \times w(i,j)\right) \bmod \phi(i,j). \quad (14)$$

Step 6: Recover the original image I by the original LSB image I_l to the MSB image I_h'. I_h' is the same as I_h because that the watermark is not embedded into the MSBs image I_h.

$$I = I_h' + I_l = I_h + I_l. \quad (15)$$

Because the watermark is embedded into the LSB image I_l instead of the MSB image I_h, as long as the watermarked image is not illegally altered, the final visual perception factor and the adaptive advisor calculated in the image recovery phrase are the same as the ones obtained in the watermark embedding process. Therefore, the original image can be perfected recovered without distortion.

To detect the presence of the watermark, we adopt the similar watermark detection method in ref. [22]. The correlation detector can be written as

$$\Lambda = \frac{1}{mn} \sum_{i=1}^{m} \sum_{j=1}^{n} \left(I_l'(i,j) - \overline{I_l}\right) \times w(i,j). \quad (16)$$

where $\overline{I_l} = \frac{1}{mn} \sum_{i=0}^{m-1} \sum_{j=0}^{n-1} I_l'(i,j)$ (for more details see [22]).

The above-mentioned algorithm only can detect the presence of the watermark in test images. In fact, it only has 1 bit secret message to be hidden. To obtain more payload capacity, we can divide the LSB image I_l into blocks with size of $c \times c$ (e.g. $c = 16$) to get LSB image blocks $B_l(u,v)$. So, different watermark signal can be embedded into different LSB image blocks. At last, we can use similar correlation detector described in (16) to detect the presence of the watermark in different LSB image blocks $B_l(u,v)$. Furthermore, to further enhance hiding capacity, we can apply the presented algorithm to an image more than once for multiple-layer embedding.

4. Experimental Results and Performance Analysis

In this section, the proposed reversible watermarking algorithm has been applied to many different types of images with different characteristics. We choose some 512×512 8-bit gray-scale images shown in Fig. 3 as the test sample. The watermark signal is produced by a pseudo random sequence initiated by the secret key k. In all experiments, we set the MSBs number for visual perception calculation $r = 4$, and the slide window size in (2) $l = 2$.

4.1 Transparency

During modulo-256 addition, a very bright pixel with a large gray value (close to 256) will possibly be changed to a very dark pixel with a small gray value (close to 0), and vise versa. As a result, the marked images generated by the modulo-256 addition based lossless watermarking algorithms usually suffer from salt-and-pepper noise. The salt-and-pepper noise becomes severe for those images that contain a number of dark and bright pixels (e.g. medical images as shown in Fig. 4a and Fig. 4b). Fig. 4 shows the test results of lossless data hiding scheme based on modulo-256 addition (called the M2A method) [18] with watermark strength of 10, where percentage of watermarked pixel is 100. From Fig. 4, it is easy to notice that the annoying salt-and-pepper noise which heavily influences the visual quality of the marked images. Especially, the peak signal to noise ratios (PSNR) of the marked image shown in Fig. 4a and Fig. 4b are as low as 6.9803 dB and 18.9180 dB respectively.

Fig.5 shows the experimental results of adopting the AMA method when all the pixels are watermarked. There are no visible perceptible artifacts in Fig. 5, indicating that a significant performance improvement has been achieved as compared with ref. [18]. This is because our lossless watermarking approach uses adaptive modular arithmetic rather than modulo-256 addition.
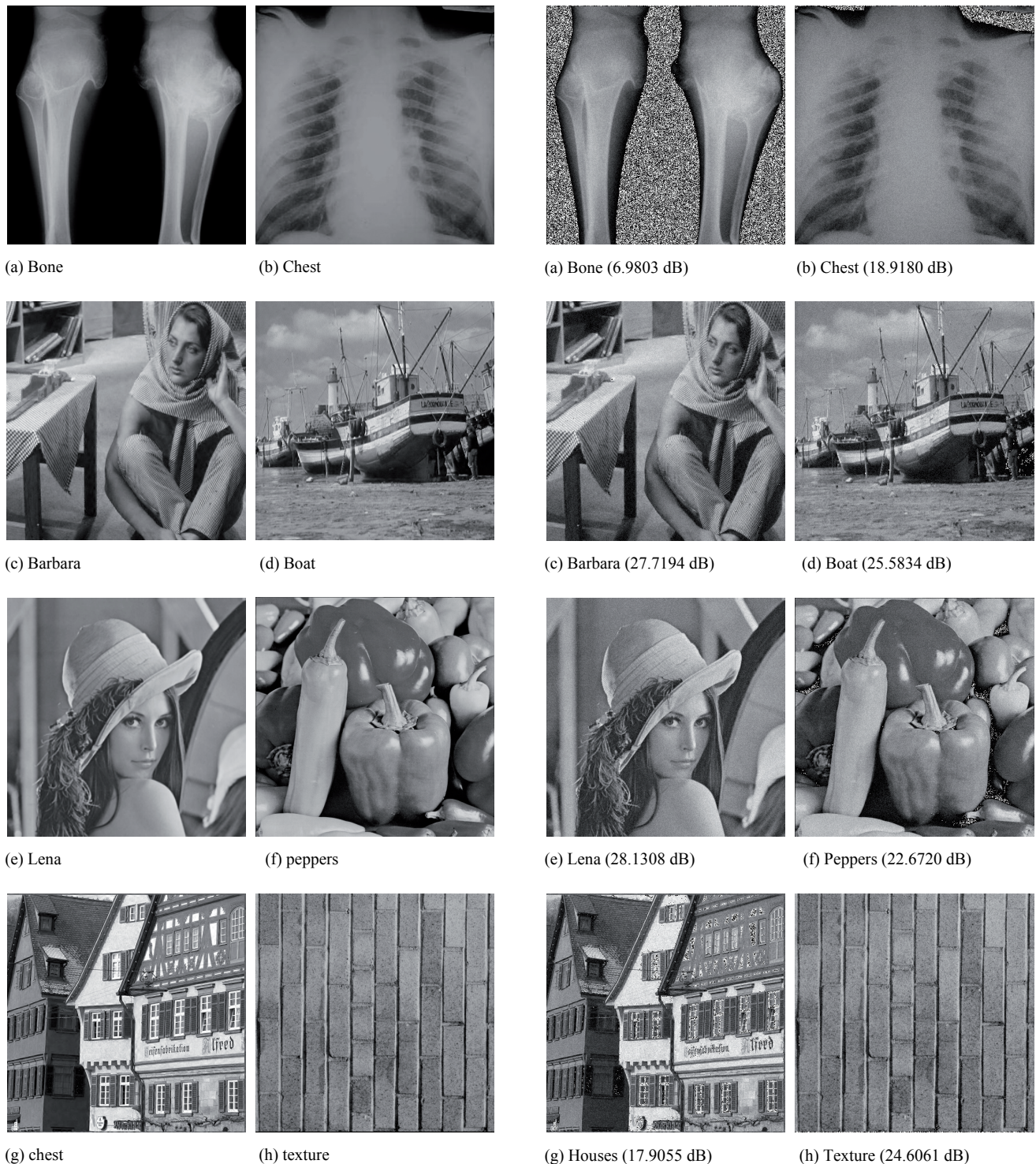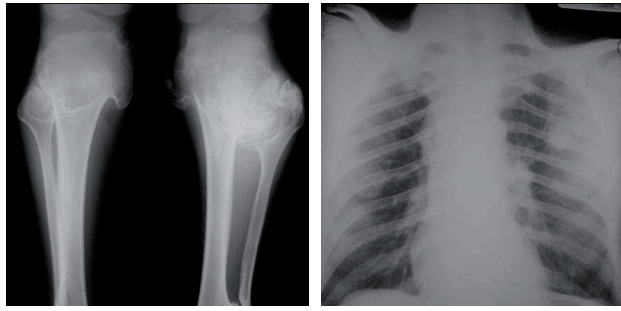
(a) Bone

(b) Chest

(c) Barbara

(d) Boat

(e) Lena

(f) peppers

(g) chest

(h) texture

Fig. 3. Some test image examples.

In particular, the effectiveness of the final visual perception factor can be illustrated by difference images between the original images and its corresponding watermarked ones (generated by the presented algorithm) with luminance enhancement by 15 times as shown in Fig. 6. It is clear that the watermark is mainly embedded into highly activated image regions, indicating that the watermark embedding is adaptive to the original image characteristics. This may also be attributed to the full use of the visual perception characteristics.

(a) Bone (6.9803 dB)

(b) Chest (18.9180 dB)

(c) Barbara (27.7194 dB)

(d) Boat (25.5834 dB)

(e) Lena (28.1308 dB)

(f) Peppers (22.6720 dB)

(g) Houses (17.9055 dB)

(h) Texture (24.6061 dB)

Fig. 4. Marked images using the M2A method.

4.2 Performance on Distortion

In our experiments, the peak signal noise ratio (PSNR) is used to evaluate the visual quality of the watermarked image. The PSNR values of embedded images for different types of images with different percentage of watermarked pixel are shown in Fig. 7. We can easily see that the PSNR value can reach as high as at least 33 dB with 100 percentage of watermarked pixel. The proposed algorithm has the

(a) Bone (41.9654 dB)

(b) Chest (42.0136 dB)

(c) Barbara (35.6067 dB)

(d) Boat (37.6092 dB)

(e) Lena (38.1172 dB)
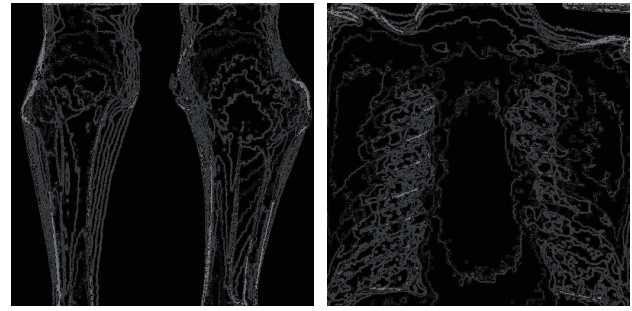
(f) Peppers (38.1604 dB)

(g) Houses (33.7903 dB)

(h) Texture (35.4348 dB)

Fig. 5. Marked images using the proposed method.

best performance for Lena image, which it is able to achieve good watermarked image quality of 52.2426 dB with 10 percentage of watermarked pixel. The results demonstrate that the proposed algorithm has good invisibility for different types of images.

To objectively judge the performance of the proposed algorithm, we can deduce the expectation of the PSNR value of stego-image generated by the proposed algorithm.
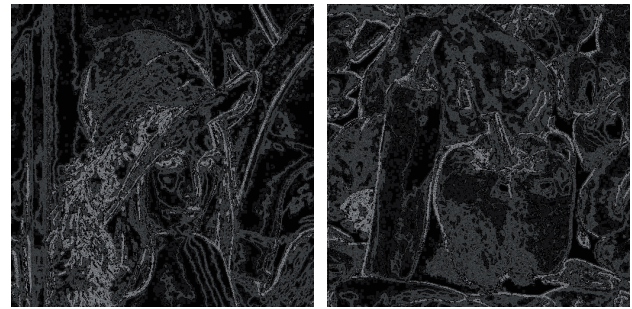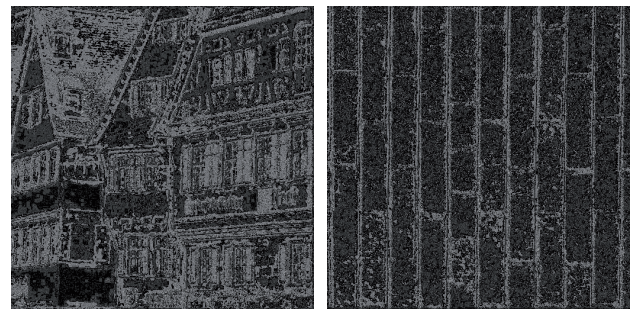

(a) Bone

(b) Chest

(c) Barbara

(d) Boat

(e) Lena

(f) Peppers

(g) Houses

(h) Texture

Fig. 6. Difference images with luminance enhancement by 15 times.

Given the MSBs number r for visual perception calculation, the adaptive LSBs number $\lambda(i,j)$ in pixel $I(i,j)$ for modular addition operation is considered to obey uniform distribution over range $[1, 8 - r]$ for an ideal natural image. So, the expectation of the adaptive LSBs number $\lambda(i,j)$ can be calculated by the formula,

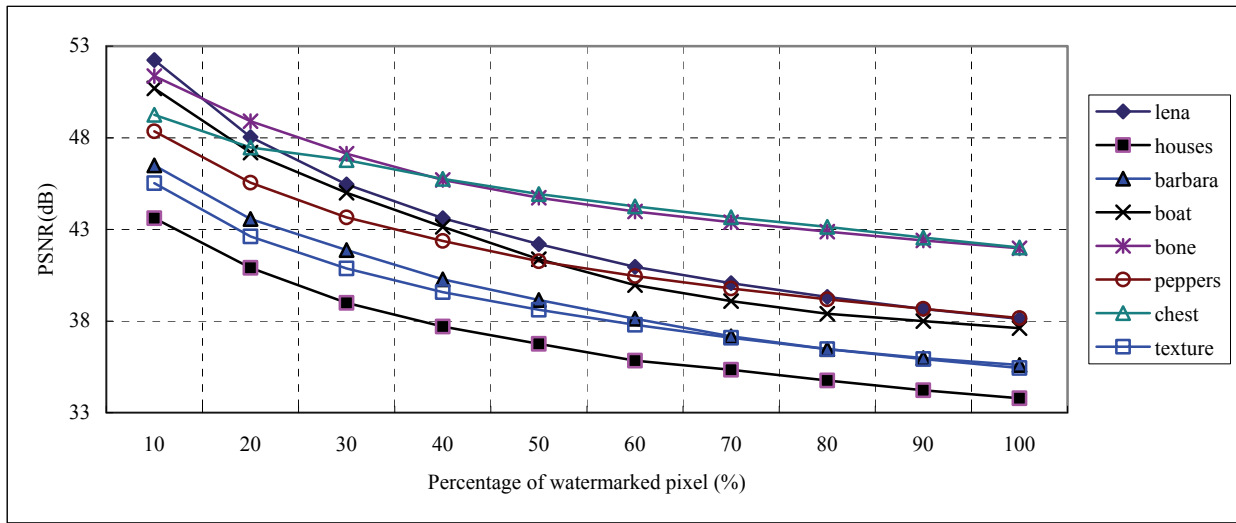$$E\left(\lambda(i,j)\right) = \frac{1+8-r}{2} = \frac{9-r}{2}. \tag{17}$$

Fig. 7. Distortion versus percentage of watermarked pixel performance using the proposed algorithm for different types of images.

r	Percentage of watermarked pixel η (%)									
	10	20	30	40	50	60	70	80	90	100
1	39.3802	36.3699	34.6090	33.3596	32.3905	31.5987	30.9292	30.3493	29.8378	29.3802
2	42.6337	39.6234	37.8625	36.6131	35.6440	34.8522	34.1827	33.6028	33.0913	32.6337
3	46.0001	42.9898	41.2288	39.9795	39.0104	38.2185	37.5491	36.9692	36.4576	36.0001
4	49.5402	46.5299	44.7690	43.5196	42.5505	41.7587	41.0892	40.5093	39.9977	39.5402
5	53.3596	50.3493	48.5884	47.3390	46.3699	45.5781	44.9086	44.3287	43.8172	43.3596
6	57.6605	54.6502	52.8893	51.6399	50.6708	49.8790	49.2095	48.6296	48.1180	47.6605
7	62.9020	59.8917	58.1308	56.8814	55.9123	55.1205	54.4510	53.8711	53.3596	52.9020

Tab. 2. Expected PSNR value versus percentage of watermarked pixel using the proposed algorithm with different MSBs number r.

Let $\delta(i,j) = x'(i,j) - x(i,j)$ be the hidden error between $x'(i,j)$ and $x(i,j)$. When $E(\lambda(i,j))$ LSBs in each pixel $I(i,j)$ are used to data hiding, $\delta(i,j)$ can be also considered to obey uniform distribution over range $[-2^{E(\lambda(i,j))}+1, 2^{E(\lambda(i,j))} - 1]$ if the watermark signal obeys uniform distribution. So, we can conclude that the hidden error $\delta(i,j)$ has zero mean. Finally, the expected mean square error (MSE) caused by the presented scheme can be computed as follows,

$$
\begin{aligned}
MSE &= E\left(\delta^2(i,j)\right) \\
&= D\left(\delta(i,j)\right) - \left(E\left(\delta(i,j)\right)\right)^2 \\
&= D\left(\delta(i,j)\right) \\
&= \frac{\left(2^{E(\lambda(i,j))} - 1 - \left(-2^{E(\lambda(i,j))} + 1\right)\right)^2}{12} \\
&= \frac{\left(2^{E(\lambda(i,j))} - 1\right)^2}{3} \\
&= \frac{\left(2^{\frac{9-r}{2}} - 1\right)^2}{3}.
\end{aligned}
\tag{18}
$$

Finally, given the percentage of watermarked pixel η, $0 < \eta \le 1$, the expectation of PSNR value obtained by the proposed scheme can be get by the following formula,

$$
PSNR_e = 10\log_{10}\left(\frac{255^2}{\eta \times MSE}\right). \tag{19}
$$

Tab. 2 lists the expected PSNR value versus percentage of watermarked pixel using the proposed algorithm with different MSBs number r for visual perception calculation. It can be seen that the proposed algorithm can achieve satisfactory expected PSNR value for different percentage of watermarked pixel with different MSBs number r. For example, for $r = 4$, it can obtain the stego-image quality of 46.0001 dB with $\eta = 10\%$, and 39.5402 dB with $\eta = 100\%$.

4.3 Capacity versus Distortion Performance Comparisons

We also compared the proposed AMA method with the existing reversible watermarking algorithms in terms of pure payload versus the stego-image quality. Overall com-

parison among various reversible watermarking schemes on two typically different images, Lena and Bone is listed in Tab. 3. Note that the host image is divided into image sub-blocks with the same size of 16×16 for different reversible watermarking schemes. By embedding the same size payload, the watermarked images by our AMA method have better watermark transparency than the other lossless watermarking algorithms [18], [20] and [21] do. Especially, for $r = 4$, the PSNR value achieved by the presented algorithm is about 9.9864 higher than that by the modulo-256 addition based method [18].

Methods	Payload (bits)	PSNR of watermarked image (dB)	
		Lena	Bone
AMA	1024	38.1172	41.9654
M2A [18]	1024	28.1308	6.9803
C. D. Vleeschouwer et al.'s [20]	1024	31.2374	25.4752
S. Weng et al.'s [21]	1024	34.3651	32.9685

Tab. 3. Overall comparison between other reversible watermarking methods [18, 20, 21] and our scheme.

5. Conclusion

By exploiting the luminance masking, texture masking and edge masking based on the image features, a novel spatial visual perception model is created, and then an adaptive divisor for modular arithmetic is deduced on the basis of the model. At last, a novel reversible watermarking scheme is presented by using visual perception model and adaptive modular arithmetic. The proposed algorithm is able to eliminate the salt-and-pepper visual artifacts in the watermarked images effectively, and achieves better transparency in contrast with some existing reversible watermarking algorithms. Especially, the proposed algorithm can obtain about 9.9864 dB higher PSNR value than modulo-256 addition based reversible watermarking schemes.

Acknowledgements

References

[1] ZHANG, X., WANG, S. Statistical fragile watermarking capable of locating individual tampered pixels. *Signal Processing Letters*, 2007, vol. 14, no. 10, p. 727-730.

[2] HO, A. T. S., XUNZHAN ZHU, JUN SHEN, et al. Fragile watermarking based on encoding of the zeroes of the Z-transform. *IEEE Transactions on Information Forensics and Security*, 2008, vol. 3, no. 3, p. 567-569.

[3] XIANG SHIJUN, KIM, H. J., HUANG, J. W. Invariant image watermarking based on statistical features in the low-frequency domain. *IEEE Transaction on Circuits and Systems for Video Technology*, 2008, vol. 18, no. 6, p. 777-790.

[4] VEYSEL ASLANTAS A singular value decomposition based image watermarking using genetic algorithm. *AEU-International Journal of Electronics and Communications*, 2008, vol. 62, no. 5, p. 386-394.

[5] FRIDRICH, J., GOLJAN, M., DU, R. Lossless data embedding for all image formats. In *Proc. SPIE Photonics West, Electronic Imaging 2002, Security and Watermarking of Multimedia Contents*. California: SPIE Press, 2002, p. 572-583.

[6] HSIEN-WEN TSENG, CHI-PIN HSIEH Reversible data hiding based on image histogram modification. *Imaging Science Journal*, 2008, vol. 56, no. 5, p. 271-278.

[7] YUN Q. SHI, ZHICHENG NI, DEKUN ZOU et al. Lossless data hiding: fundamentals, algorithms and applications. In *Proc. the 2004 International Symposium on Circuits and Systems (ISCAS 2004)*, New York: IEEE Press, 2004, p. 33-36.

[8] BARTON, J. M. Method and apparatus for embedding authentication information within digital data. *U.S. Patent 5,646,997*, 1997.

[9] CELIK, M. U., SHARMA, G., TEKALP, A. M. et al. Lossless generalized-LSB data embedding. *IEEE Transactions on Image Process*, 2005, vol. 14, no. 2, p. 253-266.

[10] AWRANGJEB, M., KANKANHALLI, M. S. Reversible watermarking using a perceptual model. *Journal of Electronic Imaging*, 2005, vol. 14, no. 1, p. 1-8.

[11] FRIDRICH, J., GOLJAN, M., DU, R. Lossless data embedding: new paradigm in digital watermarking. *EURASIP Journal of Signal Processing*, 2002, vol. 2002, no. 2, p. 185–196.

[12] TIAN, J. Reversible data embedding using a difference expansion. *IEEE Transactions on Circuits System Video Technology*, 2003, vol. 13, no. 8, p. 890-896.

[13] DILJITH M. THODI, JEFFREY J. RODRÍGUEZ. Expansion embedding techniques for reversible watermarking. *IEEE Transactions on Image Processing*, 2007, vol. 16, no. 3, p. 721-730.

[14] KURIBAYASHI, M., MORII, M., TANAKA, H. Reversible watermark with large capacity based on the prediction error expansion. *IEICE Transactions on Fundamentals of Electronics, Communications and Computer Sciences*, 2008, vol. E91-A, no. 7, p. 1780-1790.

[15] KUO, W. C., JIANG, D. J., HUANG, Y. C. Reversible data hiding based on histogram. In *Proc. the 3rd International Conference on Intelligent Computing*. Berlin/Heidelberg: Springer, 2007, LNAI 4682, p. 1152–1161.

[16] TSAI, P., HU, Y. C., YEH, H. L. Reversible image hiding scheme using predictive coding and histogram shifting. *Signal Processing*, 2009, vol. 89, no. 6, p. 1129-1143.

[17] KYUNG-SU KIM, MIN-JEONG LEE, HAE-YEOUN LEE, HEUNG-KYU LEE Reversible data hiding exploiting spatial correlation between sub-sampled images. *Pattern Recognition*, 2009, vol. 42, no. 11, p. 3083-3096.

[18] HONSINGER, C. W., JONES, P. W., RABBANI, M., STOFFEL, J.C. Lossless recovery of an original image containing embedded data. *US Patent no. 6278791*, August 2001.

[19] MACQ, B. Lossless multiresolution transform for image authenticating watermarking. In *Proceedings of the European Signal Processing Conference (EUSIPCO 2000)*. Tampere (Finland), September 2000, p. 533-536.

[20] VLEESCHOUWER, C. D., DELAIGLE, J. F., MACQ, B. Circular interpretation of bijective transformations in lossless watermarking for media asset management. *IEEE Transactions on Multimedia*, 2003, vol. 5, no. 1, p. 97-105.

[21] WENG, S., ZHAO, Y., PAN, J. S. Reversible watermarking based on improved patchwork algorithm and symmetric modulo operation. In *Proc. 9th International Conference on Knowledge-Based Intelligent Information and Engineering Systems (KES 2005)*. Berlin/Heidelberg: Springer, 2005, LNCS 3684, p. 317-323.

[22] MOON HO LEE, KORZHIK, V., MORALES-LUNA, G. et al. Image authentication based on modular embedding. *IEICE Transactions on Information and Systems*, 2006, vol. E89-D, no. 4, p. 1498-1506.

[23] BENDER, W., GRUHL, D., MORIMOTO, N., AIGUO LU Techniques for data hiding. *IBM Systems Journal*, 1996, vol. 35, no. 3-4, p. 313-336.

[24] HUIYAN QI, DONG ZHENG, JIYING ZHAO Human visual system based adaptive digital image watermarking. S*ignal Processing*, 2008, vol. 88, no. 1, p. 174-188.

[25] LEVICKÝ, D., FORIŠ, P. Human visual system models in digital image watermarking. *Radioengineering*, 2004, vol. 13, no. 4, p. 38-43.

[26] QIANG LI, CHUN YUAN, YU-ZHUO ZHONG Adaptive DWT-SVD domain image watermarking using human visual model. In *Proc. 9th International Conference on Advanced Communication Technology*. New York: IEEE Press, 2007, vol. 3, p. 1947-1951.

[27] PARKER KRISTEN, M., FOWLER JAMES, E. Redundant-wavelet watermarking with pixel-wise masking. In *Proc. the 2005 International Conference on Image Processing*. New York: IEEE Press, 2005, vol. 1, p. 685-688.

[28] BARNI, M., BARTOLINI, F., PIVA, A. Improved wavelet-based watermarking through pixel-wise masking. *IEEE Transactions on Image Processing*, 2001, vol. 10, no. 5, p. 783-791.

[29] CAI, Y. A novel imaging system for tongue inspection. In *Proc. the 19th IEEE Conference on Instrumentation and Measurement Technology*. New York: IEEE Press, 2002, vol. 1, p. 159-163.

[30] CHEN, C. H., WENG, M. F., JENG, S. K., CHUANG, Y. Y. Emotion-based music visualization using photos. In *Proc. the 24th International Conference on MultiMedia Modeling*. Germany, Berlin/Heidelberg: Springer-Verlag, 2008, LNCS 4903, p.358-368.

[31] LEVI, D. M., HARWERTH, R. S., PASS, A. F. et al. Edge sensitive mechanisms in humans with abnormal visual experience. *Exp. Brain Res.*, 1981, vol. 43, p. 270-280.

About Authors ...

Hengfu YANG was born in Hunan, China, 1974. He received the M.S. degree in Computer Application from Guizhou University, China, in 2003. He is currently pursuing a Ph.D. degree in Computer Application at School of Computer and Communication from Hunan University, China. His research interests include Multimedia, Image Processing, Digital Watermarking, and Information Hiding.

Xingming SUN was born in Hunan, China, 1963. He received the B.S. degree in Mathematics from Hunan Normal University, China, in 1984, the M.S. degree in Computing Science from Dalian University of Science and Technology, China, in 1988, and the Ph. D. degree in Computing Science from Fudan University, China, in 2001. He is currently a Professor in School of Computer and Communication, Hunan University, China. His research interests include Network & Information Security, Digital Watermarking, Wireless Sensor Network Security, and Natural Language Processing.

Guang SUN was born in Shandong, China, 1973. He received the M.S. degree in Software Engineering, from Hunan University, China, in 2005. He is currently a Ph.D. candidate in the School of Computer and Communication at Hunan University, China. His research interests include Network & Information Security, Software Watermarking, Software Birthmarking.

Zuwei TIAN was born in Hunan, China, 1973. He received the M.S. degree in Computer Software and Theory from National University of Defense Technology, China, in 2004. He is currently pursuing a Ph.D. degree in Computer Application at School of Computer and Communication from Hunan University, China. His research interests include compilers principles, Information Security, Software Watermarking.